The globular cluster system around the low-luminosity S0 galaxy NGC 7457

S. Chapelon[1], **V. Buat**[1,2], **D. Burgarella**[1], and **M. Kissler-Patig**[3,⋆]

[1] IGRAP, Laboratoire d'Astronomie Spatiale du CNRS, B.P. 8, F-13376 Marseille Cedex 12, France
[2] Laboratoire des interactions photons-matière, Faculté des Sciences de Saint Jérôme, F-13397 Marseille Cedex 20, France
[3] European Southern Observatory, Karl-Schwarzschild-Strasse 2, D-85748 Garching, Germany

Abstract. We investigate the globular cluster system around the low-luminosity S0 galaxy NGC 7457 with deep B, V, I photometry. From the V photometry the total number of globular clusters around the galaxy is estimated to be 178 ± 75. The specific frequency is estimated to be $S_N = 2.7 \pm 1.1$ adopting $M_V = -19.55$ mag for the galaxy.

We select 89 globular cluster candidates on the basis of their colors (B-I, V-I and B-V). The B-I and V-I color distributions are found unimodal with a mean metallicity $[Fe/H] \sim -1$ dex. Nevertheless the width of the B-I color distribution is found larger than that expected for a single population of globular clusters and is consistent with the presence of more than one population. If the latter is the case, the two peaks would not be detected in B-I because of the small statistics and/or a small difference in the mean metallicity of the two populations. No metal poor globular clusters similar to those of the Milky Way halo are detected around NGC 7457.

Key words: galaxies: elliptical and lenticular, cD – galaxies: individual: NGC 7457 – galaxies: star clusters

1. Introduction

The globular clusters (GCs) are among the oldest known objects in the Universe and can be considered as fossils of the formation of galaxies. GCs are simple coeval stellar systems which formed on a very short timescale during phases of intense star formation in galaxies. They are therefore more easily understood than mixed stellar field populations in a galaxy. The presence of globular cluster systems (GCSs) around most of the galaxies as well as the well known correlations found between some of their characteristics and those of the parent galaxies suggest that the formation of a galaxy and of its GCS are closely related (e.g. Harris 1991, Djorgovski & Santiago 1992).

The alternative scenarios for the formation of early-type galaxies can be divided into two classes: the classical, long-lived scenario of a monolithic collapse which occurred in the

early times of the Universe (e.g. Larson 1975) and the scenario issued from the hierarchical models of galaxy formation where the galaxies are formed through galaxy mergers (Kauffmann 1996, Baugh et al. 1998). During the unique collapse or for each major merging involving gas rich components, an intense star formation is expected with the likely formation of GCs. Indeed, it has been verified by the discovery of numerous proto-globular clusters by the Hubble Space Telescope in recently merging galaxies (and starbursting galaxies) in addition to the old ones from the progenitors (Schweizer 1997 for a review): it demonstrates that GCs trace the major events in the star formation of the parent galaxy.

The consequences of the latter scenario on the GCSs have been extensively investigated by Ashman & Zepf (1992). To date the case of the *brightest* elliptical galaxies located in rich clusters is by far the best studied. A simple monolithic formation of these galaxies seems now to be ruled out by the observation of several sub-populations of GCs around these objects, indicating a more complex formation (e.g. Geisler et al. 1996, Forbes et al. 1997). Traces of merging is very frequent in these systems and merging has probably played a role in the galaxy formation and/or evolution. Recent spectroscopic studies of GCs around NGC 1399 (Kissler-Patig et al. 1998a) and M 87 (Cohen et al. 1998) show that they probably formed massively in the early phases of the formation of these galaxies with a small contribution of recent events. However the case of cluster ellipticals may well not be appropriate to disentangle the models of galaxy formation since the hierarchical models also predict that the cluster ellipticals formed at relatively high redshift (e.g. Kauffmann 1996).

In fact the case of field galaxies seems more interesting since the predictions of each model differ significantly for this class of objects. The hierarchical models predict their formation in recent dissipational mergers of gas-rich structures (e.g. Baugh et al. 1998) which differ a lot from an early unique collapse. Early-type field galaxies with intermediate or low-luminosity are even more interesting. They might be the product of disk galaxies smaller than those involved in the formation of bright ellipticals (Kauffmann & Charlot 1998). Indeed they generally exhibit a disky structure which is consistent with a formation in a dissipational merger of gas rich systems (Faber et al. 1997,

Table 1. General data for the target galaxy, NGC 7457 from the LEDA database (http://www-obs.univ-lyon1.fr/leda/). The B and V magnitudes are the total magnitudes B_T and V_T from the LEDA database corrected by us for Galactic extinction with $A_G(B) = 4.1 \times E(B - V)$ and $A_G(V) = 3.1 \times E(B - V)$ and E(B-V)=0.0525 from Burstein & Heiles (1984). V is the heliocentric velocity. The distance modulus is calculated with the heliocentric velocity corrected for the Local Group infall onto the Virgo cluster and assuming $H_0 = 75$ km/s/Mpc (Paturel et al. 1997).

Name	RA(2000)	DEC(2000)	l	b	Type	D_{25}(arcmin)	V(km/s)	B	V	distance modulus
NGC 7457	23 00 59.9	30 08 39	96.22	-26.9	E-S0	3.98	813	11.87	11.04	30.59

Bender 1997) nevertheless the presence of gas during the merging is crucial to form new stars.

Unfortunately, the low-luminosity isolated early-type galaxies are by far less studied than the bright cluster ellipticals. In general they show no obvious hint of a past merger event (Kissler-Patig 1997). Until now, the few photometric studies of the GCSs around low-luminosity early-type galaxies are compatible with a single population and no complex formation (Kissler-Patig et al. 1998b). But in most cases the low sensitivity of the colors used to estimate parameters like metallicity or age prevents a definitive conclusion.

In this paper we present the study of the GCS of the isolated, low-luminosity S0 galaxy NGC 7457. It is a disky galaxy (Michard & Marchal 1994) and its central light distribution is fitted by a power-law without evidence for the presence of a core (Lauer et al. 1991). This galaxy does not show any trace of past interactions or merging (Schweizer & Seitzer 1992). Nevertheless a steep central power-law in a disky galaxy can be the consequence of dissipative merging of gaseous galaxies (Bender 1997). Therefore the GCS around NGC 7457 may well have kept some traces of some merger events. It is in this context that we have undertaken the study of GCS around this galaxy.

The main characteristics of NGC 7457 are presented in Table 1. Deep B, V and I photometry will allow us to investigate the luminosity function of the GCS around this galaxy, to estimate the total number of GCs and the specific frequency and to study the color distribution of the GCs.

2. Observations and data reduction

2.1. Description of the data

The B, V and I images were obtained at CFHT with the MOS instrument. A summary of the exposures is given in Table 2. The size of the field is 10×10 arcmin^2 with a pixel size of 0.44''. The equivalent exposure times are 10800 seconds in B, 4800 seconds in V and 2400 seconds in I with a seeing of 1.25'', 1.04'' and 1.11 '' respectively.

After having corrected all the images from bias and flat field, we combined the frames for each filter using a median algorithm to remove the cosmic rays and reduce the background noise. The galaxy profile has been next subtracted to perform a more reliable photometry near the central parts of the galaxy. The profile has been flattened by an iterative median-filter operation with a 15×15 pixels window. This smoothed frame was subtracted from the original picture. Fig. 1 is the final V picture on which photometry has been performed.

Table 2. Summary of the observations of the globular cluster system of NGC 7457 at CFHT with the MOS instrument.

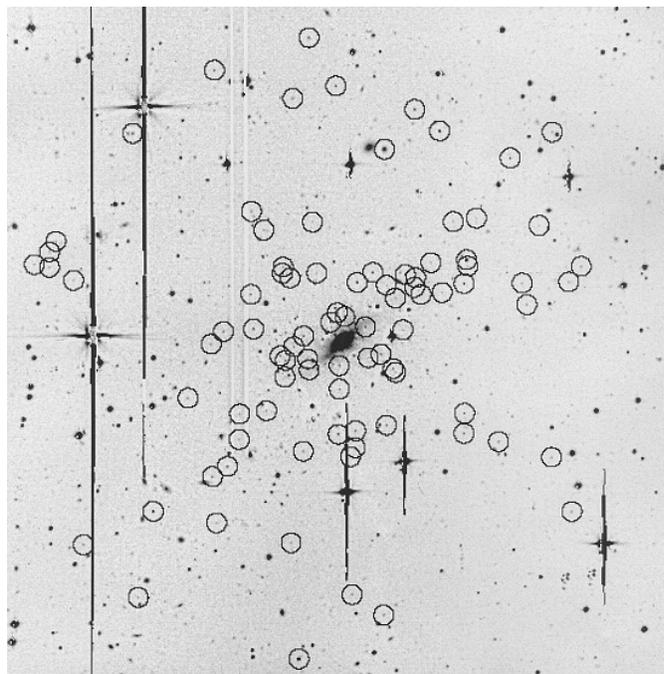| Date	Filter	Exposure time	Number of exposures
09/04/97	B	1200s	5
09/04/97	I	300s	3
09/04/97	V	600s	4
09/05/97	I	300s	4
09/05/97	V	600s	4
09/05/97	B	1200s	4

Fig. 1. The globular cluster system around NGC 7457 in the V band. The galaxy profile has been subtracted. The 89 globular cluster candidates are marked with a circle. North is up and East on the left of the figure.

The detection has been performed in the V band since the observations are far deeper than in the I band and somewhat deeper than in the B band. This has been done using the DAOPHOT software in IRAF. 846 objects have been detected at a 6σ level above the local background. Such a high level of detection has been chosen since we wanted to keep only objects with accurate photometry measurements. A standard selection has been applied on the parameters "sharpness" and "roundness" given

Table 3. Completeness percentages for the B, V and I observations as a function of the magnitude of the point sources.

Magnitude	V band	I band	B band
21.0		94.2	
21.5		95.6	
22.0		92.6	
22.25		81.6	
22.5	95.2	34.0	
23.0	93.8		94.8
23.5	92.2		91.6
23.75	85.8		78.6
24.0	37.4		35.2

by the software. Finally we discarded some objects by visual inspection.

The detection in the B and I frames was made by searching by position for objects matching the V detections. Photometry was done in the three bands with the PHOT software and only measurements with a photometric error lower than 0.2 mag have been considered. From the 846 objects detected in V, 844 have a V magnitude ($\langle\sigma(V)\rangle = 0.04$ mag), 763 have been measured in I ($\langle\sigma(I)\rangle = 0.03$ mag) and 698 in B ($\langle\sigma(B)\rangle = 0.07$ mag).

2.2. The photometric zero-point

The calibration in the three bands was done using 2 fields (including 11 standard stars) with photometric standards (SA 110 and SA 113, Landolt 1992). We determined the photometric zero-point by performing aperture photometry. The error in magnitude is estimated to be 0.02 mag in V, 0.05 mag in I and 0.05 mag in B.

A Galactic color excess E(B-V)=0.0525 has been taken in the direction of NGC 7457 from Burstein & Heiles (1984) and each magnitude has been corrected using the values $A_B = 0.22$, $A_V = 0.16$ and $A_I = 0.10$ mag calculated using the Galactic reddening curve of Pei (1992).

2.3. The completeness

The knowledge of the completeness is essential to derive a density profile and the total number of GCs around the galaxy. For each filter, we computed this completeness by adding artificial stars with the ADDSTAR routine of the DAOPHOT software. The magnitude was changed per bins of 0.25 mag or 0.5 mag. For each magnitude, 500 extra stars were added (over five runs in order to avoid crowding). The same procedure of detection as presented in Sect. 2.1 has been applied. The 50% completeness limit of a 6σ detection is found to be 23.95 mag in V, 22.45 mag in I and 23.9 mag in B. The results are summarized in Table 3.

3. The selection of globular clusters candidates

The GCs are selected on the basis of their expected range in magnitude and on their colors. Therefore, to perform such a selection, a good photometry in at least two bands is necessary.
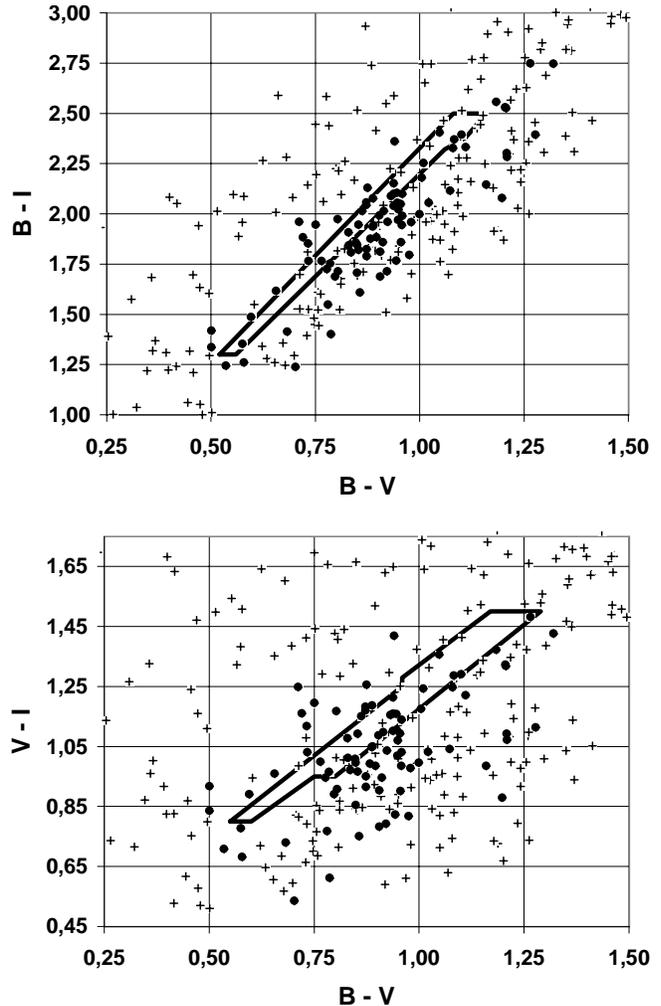

Fig. 2. Color-color plots for the globular cluster candidates around NGC 7457. The point sources objects detected in the three photometric bands are reported with crosses. The typical internal photometric error as given by DAOPHOT is 0.3 mag for each color (2σ). The solid line is the envelope found by plotting synthesis models of stellar populations (Worthey 1994) for a large range of metallicity (0.002 $Z_\odot$ to 2.5 $Z_\odot$) and age (1 Gyr to 18 Gyr). The objects whose colors are compatible with the models when accounting for the photometric error given for each measurement by DAOPHOT are marked with a filled circle. We keep only the objects selected in both color-color diagrams.

We start from the list of point-like objects detected in the V frame and for which the V and I magnitudes are measured with a photometric error lower than 0.2 mag (see Sect. 2.1). We exclude the central region of the galaxy (galactocentric distance lower than 15 arcsec) as well as the very external part of the image (galactocentric distance larger than 226 arcsec) in order to avoid too large a background contamination (see Sect. 4.1 and Fig. 3). We are left with 412 objects.

First of all, we make a selection in magnitude, keeping only objects fainter than V > 19 mag. This corresponds to 3σ above the peak of the globular cluster luminosity function (GCLF) at the distance of NGC 7457 (distance modulus of 30.59, see

Table 1), for a standard GCLF with $M_V = -7.4$ mag and $\sigma(M_V) = 1.2$ mag (Harris 1991).

    The selections in colors are made by comparing the V-I, B-V and B-I colors with the predictions of stellar population synthesis models. In Figs. 2a and b are plotted these colors together with the envelope of points generated from the models of Worthey (1994) for single stellar populations with a large range of parameters (a metallicity ranging from 0.002 $Z\odot$ to 2.5 $Z\odot$ for ages comprised between 1 Gyr and 18 Gyr and three different initial mass functions (Salpeter (exponent x=-2.35 from $M_l = 0.21$ M$\odot$ to $M_u = 10$ M$\odot$), Miller-Scalo (Miller & Scalo, 1979, with $M_l = 0.1$ M$\odot$ to $M_u = 10$ M$\odot$) and with an exponent x=-1.35 (from $M_l = 0.33$ M$\odot$ to $M_u = 10$ M$\odot$)). We select all objects whose colors are consistent with the envelope of the models adopting a 2σ uncertainty on each color given by the DAOPHOT software. We use the models of Bertelli et al. (1994): they lead to a similar selection of GC candidates. The resulting range of acceptable colors is $0.80 < V - I < 1.50$, $1.3 < B - I < 2.7$, $0.5 < B - V < 1.6$ but our selection is more refined than adopting simple color ranges since we check the compatibility of the three colors by their locus in color-color diagrams. For the objects which are not detected in B (5% of the sample) a range of plausible values for their B magnitude is estimated from the models and their V-I colors. Then we reject the objects which must be detected in B (the limiting B magnitude is taken at 23.5 mag (90% of completeness)). After these selections we are left with 89 GC candidates, out of which only 3 have no B measurement.

4. The number of globular clusters and the specific frequency

4.1. The density profile

We study the density profile of GCs using the *unselected* V detections down to V=23.9 mag, our 80% completeness limit. To compute this density profile we bin the sample in elliptical rings having the same inclination and ellipticity as NGC 7457 ($\epsilon = 0.41$ and p.a. = 130°, LEDA database). The major axis step is about 25 $''$ and the minor 15 $''$. The counts are then corrected for magnitude incompleteness. No correction for geometrical incompleteness is necessary except for the last ring (major axis from 300 to 325 $''$ from the center) for which we lack 10% of the surface because of the limited size of the observed field. We do not consider the most central part of the galaxy which is saturated (for radii smaller than 15 $''$). Inside the geometrical bins, we group the data in magnitude bins of 0.5 mag to correct for incompleteness at different magnitudes. The counts are shown in Table 4. For the first ring, we could not estimate the Poissonian error because we are too close from the center of the galaxy.

    In Fig. 3 are plotted the radial variation of the surface density, distribution for our point-like V detections together with the galactic V light profile. The background contamination can been estimated when the density profile reaches a constant value. Practically this occurs for galactocentric distances larger than 200 arcsec. The average of the counts in the five last rings (Ta-
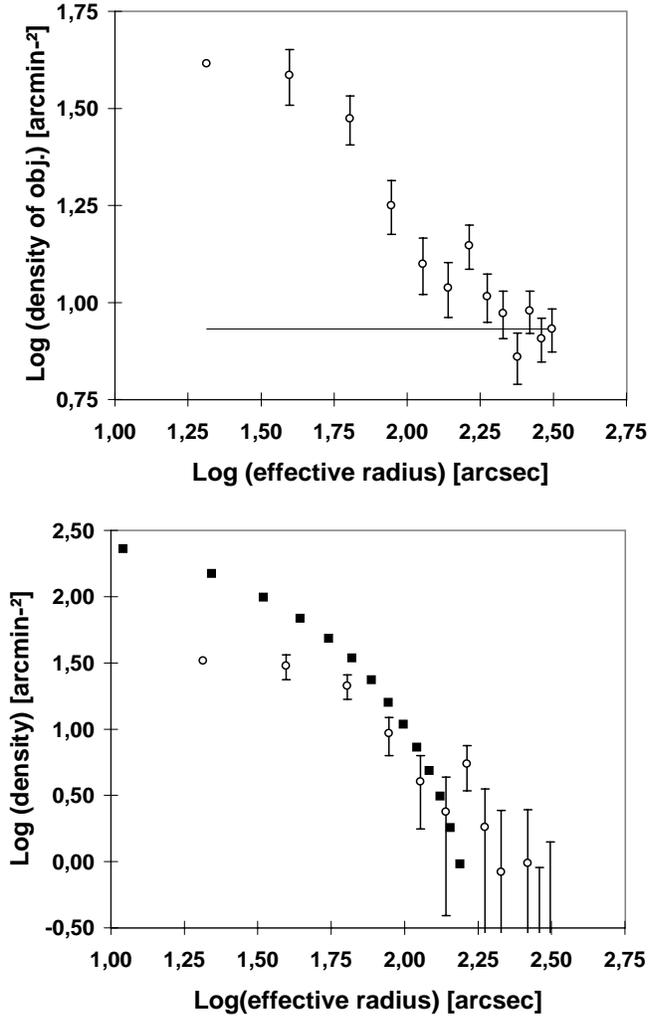

Fig. 3. Upper panel: the surface density profile (open circles) of point-like objects detected around NGC 7457 in the V frame from the values quoted in Table 4. The profile flattens at about 225 $''$ to a constant level of 8.5 ± 0.9 objects/arcmin^2 (line). Lower panel: the surface density profile of the globular cluster system (open circles) compared with the isophotal galaxy light in V plotted in arbitrary units with filled squares.

ble 4, Column 5) gives 8.5 ± 0.9 objects/arcmin^2 in agreement with the deep counts down to V = 23.9 mag, our 80% limit completeness (Peterson et al. 1979, Tyson 1988). After applying corrections for incompleteness, the total number of objects down to this magnitude is estimated to be 537 ± 38. The background is subtracted statistically over an area of 46.34 arcmin^2 (thus 394 ± 46 objects) and we are left with a total of 143 ± 60 GC candidates.

    The density profile of the GCs follows the galaxy light profile. The fit of a power-law on the profiles ($\propto r^{-\alpha}$) gives $\alpha = 2.10 \pm 0.26$ for the GC density profile and $\alpha = 2.02 \pm 0.23$ for the galaxy light profile. We used all the data points except for the first bin for which we do not estimate the error. Such a slope ($\alpha \simeq -2$) for the GC profile of NGC 7457 whose absolute V magnitude is -19.55 mag is in agreement with the correlation found between this slope and the absolute magnitude of the

Table 4. The globular cluster counts around NGC 7457. The counts are performed in elliptical rings down to a magnitude V = 23.9 mag. In Column 2 are reported the counts without any correction. In Columns 4 and 5 the counts are corrected for completeness, the quoted errors are Poissonian. In Column 6 the density of GCs is corrected for the background contamination, the quoted error accounts for the error on the counts (Column 4) and on the background (8.5 ± 0.9 objects/arcmin^2, see text).

| Ring major axis arcsec	Objects counts	Ring surface arcmin^2	Corrected counts	Surface density objects/armin^2	Density profile GCs/armin^2
15–25	8	0.21	8.5 ±?	41.3 ±?	32.7 ±?
25–50	34	0.97	37.2 ± 6.1	38.5 ± 6.3	30.0 ± 6.4
50–75	44	1.61	47.9 ± 6.9	29.8 ± 4.3	21.2 ± 4.4
75–100	37	2.25	40.1 ± 6.3	17.8 ± 2.8	9.3 ± 3.0
100–125	34	2.90	36.4 ± 6.0	12.6 ± 2.1	4.0 ± 2.3
125–150	36	3.54	38.6 ± 6.2	10.9 ± 1.8	2.4 ± 2.0
150–175	54	4.18	58.6 ± 7.7	14.0 ± 1.8	5.5 ± 2.0
175–200	46	4.83	50.0 ± 7.1	10.4 ± 1.5	1.8 ± 1.7
200–225	48	5.47	51.3 ± 7.2	9.4 ± 1.3	0.8± 1.6
225–250	41	6.11	44.3 ± 6.7	7.2 ± 1.1	-1.3 ± 1.4
250–275	60	6.76	64.3 ± 8.0	9.5 ± 1.2	1.0 ± 1.5
275–300	56	7.40	59.7 ± 7.2	8.1 ± 1.0	-0.5± 1.4
300–325	58	7.27	62.1 ± 7.9	8.5 ± 1.2	0.0± 1.4
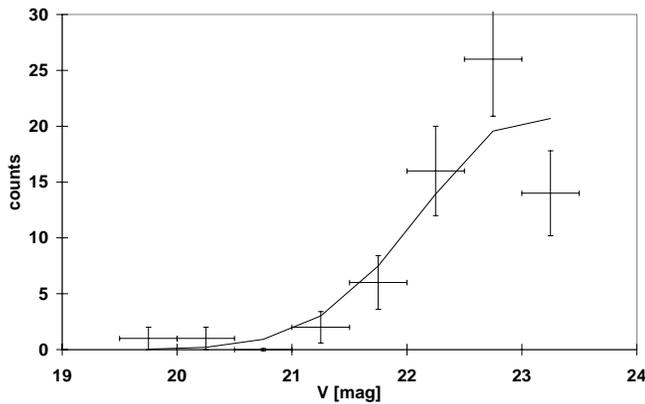
Fig. 4. The globular cluster luminosity distribution in the V band fitted by a gaussian function with mean and σ equal respectively to 23.1 mag and 0.9 mag.

parent galaxy, fainter galaxies having a steeper distribution of GCs (e.g. Harris 1991, Kissler-Patig 1997). A similar profile for the galaxy light and the GCS seems not to be the rule for bright ellipticals (e.g. Ashman & Zepf 1998) but the case of low-luminosity early-type galaxies is less clear since very few data are available for them.

4.2. The globular cluster luminosity function

To compute the globular cluster luminosity function we would need to consider only genuine GCs. To this aim, we use the GC candidates selected in Sect. 3 from V and I detections.

We have to account for incompleteness effects due to the magnitude limits in V and I. The range of V-I colors for the GC candidates is estimated from the models of Worthey namely $0.80 < V - I < 1.5$. Since the GC candidates are first detected in the V band, we apply a selection which ensures the full range

of possible V-I color for each detected candidate. With a completeness limit (50%) at 22.45 mag for I and 23.95 mag for V we are limited by the I detections and we have to truncate the sample at V=23.25 mag which is reduced to 65 GC candidates.

The GCLF is shown for V< 23.25 mag in Fig. 4. A gaussian distribution has been fitted to the bins not affected by incompleteness. The parameters of the gaussian are $M_V = 23.1 \pm 0.2$ mag for the mean and a dispersion of $\sigma_V = 0.9 \pm 0.3$ mag. The mean value that we find is fully consistent with a mean absolute magnitude $M_V = -7.4$ mag for the distance modulus of NGC 7457 (Table 1). The dispersion we find for the GCLF of NGC 7457 is marginally consistent with those found in galaxies like M 31 or the Milky Way with $\sigma_V = 1.2 \pm 0.1$ mag whereas for bright ellipticals the dispersion seems larger with $\sigma_V \simeq 1.4$ mag (e.g. Ashman & Zepf 1998).

4.3. The specific frequency

The number of GCs in an early-type galaxy has been found to scale with the parent galaxy luminosity (e.g Djorgovski & Santiago 1992). Therefore following Harris & van den Bergh (1981) the GC counts are normalized per absolute visual magnitude of $M_V = 15$ mag and a specific frequency is defined as $S_N = N \times 10^{0.4 \cdot (M_V + 15)}$ where N is the total number of GCs in the galaxy and M_V its absolute visual magnitude. S_N is a measure of the GC efficiency. S_N is found to be ~ 5 for most early-type galaxies with $-19 > M_V > -22$ although with a large dispersion. Brighter early-type galaxies exhibit in average a larger S_N, some giant ellipticals in rich clusters having a very large specific frequency $S_N > 10$ (Kissler-Patig 1997).

In the Sect. 4.1 we estimated the total number of GCs down to $M_V = 23.9$ mag. Then integrating over the entire luminosity distribution of the Sect. 4.2 we deduce a total number of 178 ± 75 clusters. This translates to a specific frequency $S_N = 2.7 \pm 1.1$ assuming an absolute V magnitude $M_V = -19.55$ mag
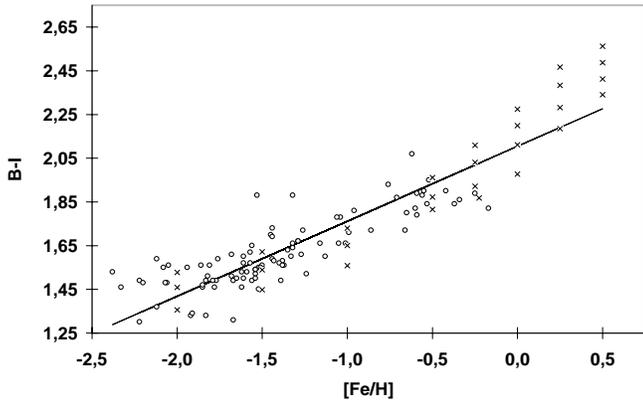
Fig. 5. B-I color versus metallicity of the MW globular clusters (open circles) together with the the results of Worthey's models for old homogeneous stellar populations (crosses). The solid line is the result of the linear regression.

Fig. 6. The histogram of the V-I color distribution for the globular clusters of NGC 7457. The typical internal photometric error is 0.10 mag as the size of the bins.

for NGC 7457. We can compute in the same way the specific frequency from the number of detected GC down to V = 23.1 mag (the turn-over of the GCLF) and, after multiplying by two, we are left with 132 ± 58 objects thus $S_N = 2.0 \pm 0.9$.

5. The color distributions of the globular clusters

Now we study the V-I and B-I color distributions of the GCs around NGC 7457 in order to search, if any, the presence of subpopulations with different metallicities. Indeed the B-I color and in a lesser extent the V-I color are sensitive to the metallicity provided that the GCs are old (> 5 Gyr). In case of old stellar populations these two colors are poor tracers of the age of the stellar populations (Worthey 1994, Kissler-Patig et al. 1998a).

First we need to calibrate the V-I and B-I colors as a function of the metallicity. Empirical relations based on the observation of the Milky Way (MW) GCs are commonly used (e.g. Couture et al. 1990) but these relations become very insecure outside the metallicity range of the MW GCs ($-2.0 \leq [Fe/H] \leq -0.5$). Kissler-Patig et al. (1998a) have extended the comparison between V-I and the metallicity deduced from spectroscopic data to higher metallicities thanks to their observations of NGC 1399 and found a flatter relation of [Fe/H] as a function of V-I than when only the MW GCs are considered. In this paper, we will adopt the relation of Kissler-Patig et al. (1998a):

$$[Fe/H] = (-4.50 \pm 0.30) + (3.27 \pm 0.32)(V - I)$$

For the relation between the B-I color and the metallicity of GCs we re-analyse the problem by using the data on the MW clusters (Harris 1996, McMaster database) together with the synthesis models of Worthey (1994) for old stellar populations (> 5 Gyr) with a large range of metallicities ($-2.0 \leq [Fe/H] \leq 0.5$). We consider only old ages for the models in order to be consistent with the age of the MW GCs. Therefore, the calibration relation will be valid for old stellar populations only (> 5 Gyr). When comparing the colors listed in Worthey (1994) with the observed MW GCs, a small shift in color is needed. Assuming an average age of 12 Gyr for the MW GCs, we get a slight correction (-0.09
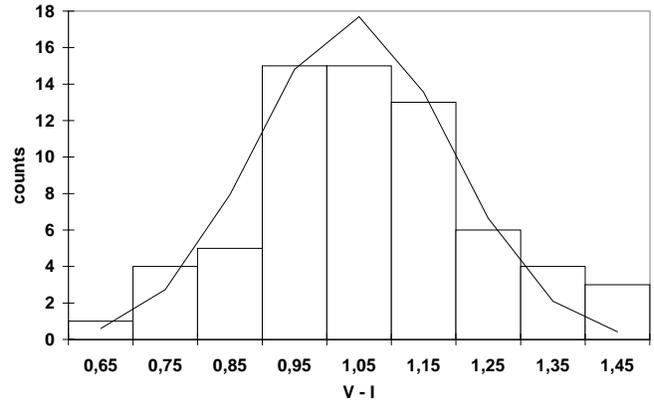
in V-I, -0.14 in B-I) to apply to the models. These corrections are in reasonable agreement with the color shifts suggested by Worthey. The data are presented in Fig. 5. A linear regression gives:

$$[Fe/H] = (-5.34 \pm 0.42) + (2.44 \pm 0.30)(B - I)$$

Given the uncertainties about these calibration relations, we have checked that our results do not depend on the exact choice of the conversion formulae. Indeed we have used different relations like those of Couture et al. (1990) for both V-I and B-I as well as the relation we find between [Fe/H] and V-I following the same method as described in the last paragraph (MW data and synthesis models).

5.1. The V-I color distribution

The V-I color histogram is reported in Fig. 6 for the sample of 65 GCs with V < 23.25 mag (see Sect. 4.2). The distribution is found unimodal using the KMM mixture-modeling algorithm (Ashman et al. 1994). The gaussian distribution fitted on the data has a mean $\langle V - I \rangle = 1.04 \pm 0.02$ mag and a standard deviation $\sigma(V - I) = 0.15 \pm 0.04$ mag. We can also estimate the mean and standard deviation using maximum likelihood estimators (Pryor & Meylan 1993), this method has the advantage of being performed without any hypothesis on the shape of the distribution. We find very similar results i.e. $\langle V - I \rangle = 1.06 \pm 0.02$ mag and $\sigma(V - I) = 0.16 \pm 0.02$ mag. Therefore the observed standard deviation is only slightly larger than the mean internal photometric error for the sample ($\sigma_{err}(V - I) = 0.1$ mag). A mean $\langle V - I \rangle = 1.04$ mag translates to $\langle [Fe/H] \rangle = -1.1$ dex. With an absolute V magnitude of -19.55 for NGC 7457 such a mean is consistent with the correlation found between the absolute magnitude of the parent galaxy and the mean metallicity of the GCSs (e.g. Ashman & Zepf 1998).

5.2. The B-I color distribution

To compute the B-I color distribution we have to select GC candidates detected in V and with a measured magnitude in I
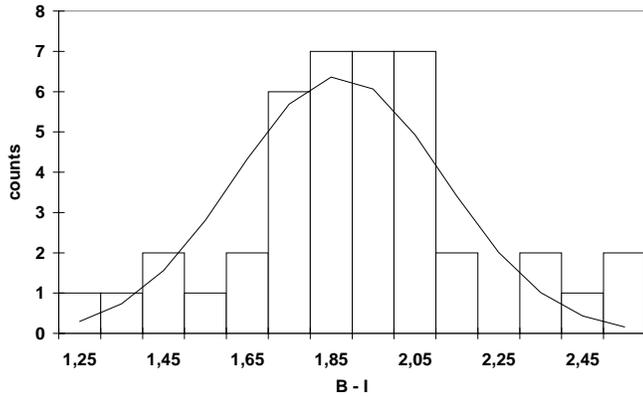
Fig. 7. The histogram of the B-I color distribution for the globular clusters of NGC 7457. The typical internal photometric error is 0.1 mag of the order of the size of the bins (0.1 mag).

and B. Given the deepness of the V detection as compared to the I and B ones, the resulted sample is equivalent to a selection based only on B and I detections. Once again we only keep objects with V > 19 mag.

We have also to be as complete as possible in the B and I bands for the analysis of the B-I color distribution. The range of B-I colors is estimated from the models of Worthey used for the selection of the GCs candidates i.e. $1.3 < B - I < 2.7$. As before, we adopt a completeness limit at 50% which corresponds to 22.45 mag in I and 23.9 mag in B. To ensure the full range of possible colors for each candidate detected in B we must truncate the sample at B=23.7 mag. The sample is reduced to 41 objects.

The B-I color histogram is reported in Fig. 7. The distribution is larger than for the V-I color but it is also found unimodal with the KMM test. Such a result is expected since Ashman et al. (1994) have shown that a bimodality cannot be easily detected with the KMM algorithm when the number of data is lower than 50 as it is the case here. The fit with a gaussian distribution gives a mean $\langle B - I \rangle = 1.87 \pm 0.02$ mag leading to a $[Fe/H] = -0.8$ dex consistent with the mean metallicity deduced from the V-I distribution given the uncertainties on the calibration relations; the observed standard deviation is $\sigma(B - I) = 0.25 \pm 0.06$ mag. Using maximum likelihood estimators we find $\langle B - I \rangle = 1.91 \pm 0.04$ mag and $\sigma(B - I) = 0.28 \pm 0.03$ mag. Therefore the observed standard deviation of the B-I distribution is larger than the mean internal error $\sigma_{\mathrm{err}}(B - I) = 0.1$ mag.

5.3. A hidden bimodality?

The V-I and B-I distributions of the GCs around NGC 7457 are found unimodal. Before discussing the implications of this result we discuss in what conditions a bimodality would be really detected. First, as already discussed it is imperative to detect more GCs and therefore to perform a deeper photometry in at least two bands. Moreover Kissler-Patig et al. (1998b) have outlined that, even if present, different populations of GCs are probably hard to discriminate in low-luminosity galaxies. A

conspiracy between age and metallicity of the two populations could mimic a unimodal V-I distribution, the V-I color being very sensitive neither to age nor to metallicity.

Another difficulty is that even if the metallicity distribution of the GCS is bimodal the two peaks might be too close to be disentangled. For example Forbes et al. (1997) have found a correlation between the mean metallicity of the metal-rich population of GCs and the luminosity of bright ellipticals whereas there is almost no correlation between the metallicity of the metal-poor GCs and the parent galaxy luminosity. If such a correlation also holds for fainter galaxies, their redder GC population will be less metal-rich and its color peak closer to that of their metal-poor GC population than it is the case in the bright ellipticals. Therefore, the two peaks in the metallicity distribution, if they exist, will be hardly detected in these galaxies.

In order to investigate more quantitatively this effect, we can try to estimate what sort of bimodality is detectable with our data. Ashman et al. (1994) have tested the bimodal detectability as a function of $\Delta\mu$, the difference between the two means divided by the standard deviation of the two sub-populations supposed to have the same dispersion. For a total number of $\sim$ 50 GCs, a bimodality is detected as soon as $\Delta\mu \geq 3$. If we adopt a typical $\sigma([Fe/H]) = 0.3$ dex for each sub-population we find $\Delta[Fe/H] \geq 0.9$ dex. However, we must note that this estimation is based on the assumption that the two sub-populations have the same number of objects. As noted by Kissler-Patig et al. (1998b, see also Sect. 6.2), if there is not an equal number of GCs in each sub-population, they cannot be separated when $\Delta[Fe/H] \sim$ 1 dex. $\Delta[Fe/H] = 0.9$ dex corresponds to $\Delta(V - I) = 0.3$ and $\Delta(B-I) = 0.4$ mag according to the calibration formulae given above. Thus, under these hypotheses, the two peaks might be separated.

A 1-dex separation seems to a rough order of magnitude of what we may find in GCSs. Indeed, in bright ellipticals the difference between the two metallicity peaks approximately or slightly larger than 1 dex (e.g. Ashman & Zepf 1998). Also, in the Milky Way, a similar gap has been measured between the metallicity of the halo and disk/bulge GCs (Armandroff & Zinn 1988).

The bottomline is that with our data we can hope to separate two peaks of a bimodal distribution similar to those found around bright ellipticals or the Milky Way provided that the two sub-populations are roughly equally represented. Any bimodal distribution with two metallicity peaks separated by less than 1 dex could not be separated.

6. Discussion

NGC 7457 is a S0 low-luminosity field galaxy. S0 galaxies are thought to be the continuation from disky ellipticals to early-type spirals in the Hubble sequence (Kormendy & Bender 1996). We can expect that S0 and disky ellipticals have been formed through similar processes. Therefore this type of galaxy is particularly interesting for testing the scenarios of galaxy formation, in particular whether these galaxies formed in a dissipational merger event (see Sect. 1).

The simple model of a spiral–spiral merger predicts several properties for the GCS of the remnant galaxy (Ashman & Zepf 1992): the newly produced GCs should rise the specific frequency by a factor of two, the new clusters and stars will be more concentrated than the GCS of the progenitors, and the new clusters should appear as a second population in the color distribution.

At face value NGC 7457 does not seem to confirm the hypothesis of a formation by spiral–spiral merging, at least when compared to the predictions of the simple model of Ashman & Zepf (1992). NGC 7457 is found to have a rather low number of GCs steeply distributed around the galaxy, and the color distribution of these GCs appears unimodal. Indeed, the specific frequency $S_N = 2.7 \pm 1.1$ is compatible with the range observed in the four studied Sa and Sab galaxies (ranging from 0.7 to 3.5 with a mean of 2.0 and a dispersion of 1.0, taken from Ashman & Zepf 1998). The surface density profile of the GCs follows the one of the stars (see Sect. 4.1). The absence of a recent merging event is suggested by the lack of any fine structure as defined by Schweizer & Seitzer (1992) for this galaxy.

However two results might constrain formation theories. First the color distributions of the GCs appear broader than for a single population such as, e.g., the Milky Way halo clusters. No clear bimodality has been detected. Nevertheless given the poor statistics it has been shown in Sect. 5.3 that it does not exclude necessarily the presence of distinct sub- populations. And, second, the peak of the color distribution appears relatively red.

6.1. A broad color distribution

Does the unimodality of the color distribution imply the absence of two distinct GC populations? In spite of the difficulties discussed in Sect. 5.3, the narrow V-I distributions found in low-luminosity early-type galaxies (Kissler-Patig et al. 1997), together with a narrow luminosity function, can be used to exclude large difference in both metallicity and age within each galaxy, and therefore a recent gas-rich merger (z<1) (Kissler-Patig et al. 1998b).

The availability of the B-I colors for the GCs of NGC 7457 allows us to go further in the analysis. Indeed the B-I color is roughly twice as sensitive to metallicity than the V-I color (Couture et al. 1990). But an intrinsic difficulty with low-luminosity galaxies is their small number of GCs. Bimodality was shown to be undetectable in a dataset containing less than 50 objects (see Sect. 5.3). Nevertheless, as we will see below, we can expect to observe some differences between the widths of a unimodal and a bimodal distributions. The dispersion in color of a "single" population of GCs can be estimated from the halo GCs of the MW. On the one hand, we can convert the metallicity dispersion into a color dispersion. With $\sigma([Fe/H]) = 0.3$ dex (Armandroff & Zinn 1988) we expect a $\sigma(V - I) \sim 0.05$ mag and $\sigma(B-I) = 0.1$ mag from the calibration relations of Sect. 5. On the other hand, we can measure the dispersion from the V-I and B-I data of the ~ 80 halo GCs in the McMaster catalog (Harris 1996), and obtain $\sigma(V - I) = 0.05 \pm 0.01$ mag and $\sigma(B - I) = 0.09 \pm 0.01$ mag in excellent agreement with the

first values. In V-I, the genuine dispersion in metallicity is extremely difficult to derive from the V-I colors, the expected dispersion being lower than the typical photometric errors of 0.1 mag. In B-I, however, typical photometric errors and intrinsic dispersion of a single population are comparable, so that several populations would broaden the color distribution to a detectable level.

In NGC 7457 the dispersion in V-I is only slightly larger than the internal error (0.15 mag against 0.10 mag) and we estimate that the true dispersion is $\sim 0.11 \pm 0.11$ mag according to the relation $\sigma_{\rm obs}^2 = \sigma_{\rm err}^2 + \sigma_{\rm true}^2$. This standard deviation in V-I translates to a $\sigma([Fe/H]) \sim 0.4 \pm 0.4$ dex when using the calibration relation given in the precedent section. The error is estimated by accounting for the uncertainties on the determination of the standard deviations and on the calibration formula given in Sect. 5. The estimate is very insecure due to the large error on $\sigma(V - I)$.

For the B-I color we find a dispersion (0.25 mag) clearly broader than the combination of a single population and photometric errors. The above relation leads to $\sigma_{\rm true} = 0.23 \pm 0.07$ mag or $\sigma([Fe/H]) = 0.6 \pm 0.2$ dex. This value is compatible with the value tentatively deduced from the V-I distribution.

Such a dispersion in metallicity seems intermediate between the one of a single population and the total dispersion of the GC populations in bright ellipticals. Indeed single populations such as the Galactic halo GCs (Armandroff & Zinn 1988), or the GCs around M 81 or M 31 (Perelmuter & Racine 1995) have $\sigma([Fe/H]) \sim 0.3$ dex; the individual components of the bimodal distribution in NGC 4472 have similar dispersions of ~ 0.38 dex in [Fe/H] (Geisler et al. 1996). In contrast, the total dispersion of the system in M87 is $\sigma([Fe/H]) = 0.65$ dex (Lee & Geisler 1993), in NGC 4472 $\sigma([Fe/H]) = 0.7$ dex (Geisler et al. 1996).

Therefore, while the distribution in metallicity of the GCs around NGC 7457 is found to be unimodal, the width of the GC metallicity distribution is compatible with the presence of different populations probably less separated in metallicity than in the giant clusters ellipticals. This suggests a significantly different chemical enrichment of the GCs in NGC 7457 than, e.g., the halo population of the Galaxy.

6.2. The mean colors of the globular clusters: implications on the scenarios of formation

With $M_V = -19.55$ and a mean metallicity of [Fe/H]$\simeq -1$ dex for its GCs, NGC 7457 follows the general trend found between the absolute magnitude of the galaxies (spirals + ellipticals) and the [Fe/H] value of their GCs (e.g. Brodie & Huchra 1991, Ashman & Zepf 1998). Nevertheless, the spirals seem to have a lower GC metallicity as compared to ellipticals of similar luminosity and the mean metallicity of [Fe/H]$\simeq -1$ dex for the GCs around NGC 7457 is consistent with the mean values found for the metallicities of the GCs around the bright elliptical galaxies ($M_V \leq -20$, e.g. Ashman & Zepf 1998).

We can also compare more quantitatively the color distribution of the GCs around NGC 7457 with that of the Galactic

globular clusters. In addition to its broad dispersion, the mean B-I color found for the GCs of NGC 7457 (B-I≃ 1.9 mag, see Sect. 5.2) is comparable to the mean of the Galactic disc/bulge GCs (B-I≃ 1.9 mag, as derived from the McMaster catalog). Moreover, Monte Carlo simulations of B-I color distributions similar to ours show that any metal-poor (B-I=1.55 mag, the mean color of the metal-poor clusters in the Galaxy) population as large as 20% to 30% of the metal-rich (B-I= 1.92 mag) one would be detected. Therefore we can conclude to the absence of any significant population of metal-poor clusters similar to that of the MW halo.

It is likely that such blue globular clusters were never present in NGC 7457 since NGC 7457 is an isolated galaxy ($\rho = 0.13$ galaxies/Mpc^3 (Tully 1988)) and shows no signs of any interaction. Thus the loss of blue GCs loss through stripping seems excluded.
The formation in a spiral–spiral merger would imply the presence of blue GCs from the progenitor spirals unless the latter did not host blue GCs like the MW. In situ formation models usually explain blue GCs as formed in the early stage of the galaxy. To fit the absence of blue clusters in such scenarios an early epoch of star formation (to enrich the gas) without any formation of GCs would be required.
We can also explore the possibility that the halo population of NGC 7457 and therefore of its progenitors in case of merging would be slightly redder than the MW one. For both the merger and accretion models, no variation of the color of the blue cluster population as a function of the parent galaxy luminosity is expected as it seems to be confirmed by Forbes et al. (1997). Indeed their mean metal-poor peak $\langle [Fe/H]\rangle = -1.2\pm 0.3$ dex obtained for bright ellipticals translates to $B - I = 1.7$ and $V\text{-}I = 1.0$ (see also Neilsen et al. 1999). An extrapolation of the trend that Forbes et al. (1997) found between the metal-rich peak and the galaxy luminosity gives $[Fe/H] \simeq -0.6$ dex and thus $B - I \simeq 1.95$, $V - I \simeq 1.2$. Such a bimodal distribution is consistent with our data since the two peaks could not be separated neither in V-I nor in B-I given the proximity of their colors (see Sect. 5.3).
Finally, the absence of blue GCs around NGC 7457 could be explained in a scenario as the one advanced by Côté et al. (1998) where a galaxy forms GCs with a mean metallicity proportional to its luminosity and gains its metal-poor GCs by accreting smaller galaxies surrounding it. In this case, the absence of a significant number of metal-poor GCs in NGC 7457 could then be due to a lack of dwarf galaxies around this isolated galaxy.

Two galaxies already were reported to lack blue globular clusters: NGC 3923 and NGC 3311. Zepf et al. (1995) have discussed various scenarios to explain the high mean metallicity ([Fe/H] = -0.56 dex) and the very few clusters with [Fe/H] < -1 dex around NGC 3923, a luminous field elliptical. They propose several explanations around the merger picture, in which the number and metallicity of the clusters formed during the merging as well as those of pre-existing clusters around the progenitors might vary. Finally more or less accretion of satellite galaxies and their metal-poor globular clusters can also modify the final color distribution of the system.

In case of NGC 3311, the central cD in the Hydra cluster, Secker et al. (1995) attribute the almost complete lack of blue GCs (less than 10% of the GCs appear to have $[Fe/H] < -1$ dex) to different history of pre-enrichment of the giant galaxy in the frame of an in situ formation of clusters.

7. Conclusions

We have studied the GCS around the low-luminosity ($M_V = -19.55$ mag) early-type galaxy NGC 7457. Several characteristics of the GCS are found typical for this type of galaxy: the specific frequency is found low with $S_N \sim 2.7$ and the GC density profile is steep and follows the stellar light of the parent galaxy. The mean metallicity of $\langle [Fe/H]\rangle \simeq -1$ dex is compatible with the correlation existing between the metallicity of the GCSs and the luminosity of the parent galaxies.

The B-I and V-I color distributions are found unimodal but the B-I distribution is much wider than expected from a typical homogeneous population of GCs and consistent with what is expected for a bimodal distribution. The poor statistics (66 globular clusters in V-I and 41 in B-I) prevents from a detection of two peaks in the metallicity distribution of the GC system if they are closer than 1 dex in [Fe/H] and/or if the two sub-populations have a very different number of objects.

Therefore our data are consistent with the presence of more than one population of GCs around NGC 7457. An alternative scenario would be a single GC population with a larger range in metallicity than found for homogeneous populations of GCs around the MW, nearby galaxies or bright ellipticals.

No significant population of metal-poor GCs similar to the halo GCs of the Galaxy is detected around NGC 7457. Several possibilities are discussed to explain this absence of globular clusters with $[Fe/H] \simeq -1.6$ dex.

Deeper photometry would be necessary to detect more GCs and to be able to identify two peaks in the metallicity distribution of the GCS. Another test of the hierarchical models of galaxy formation will be to estimate the age of the GCs since these models predict a rather recent merging for field early-type galaxies with $z < 1$. Such a determination requires spectroscopic observations of the GCs but will be difficult if the merging occurred more than 5 Gyr ago since spectroscopic indices as H_β are not sensitive to higher ages.

References

Armandroff T.E., Zinn R., 1988, AJ 96, 92
Ashman K.M., Zepf S.E., 1992, ApJ 384, 50
Ashman K.M., Zepf S.E., 1998, Globular Cluster Systems. Cambridge University Press
Ashman K.M., Bird C.M., Zepf S.E., 1994, AJ 108, 2348
Baugh C.M., Cole S., Frenk C.S., et al., 1998, astro-ph/9808209
Bender R., 1997, The Nature of elliptical Galaxies. ASP Conf Series vol. 116, 11
Bertelli G., Bressan A., Chiosi G., et al., 1994, A&AS 106, 275

Brodie J., Huchra J., 1991, ApJ 379, 157

Burstein D., Heiles C., 1984, ApJS 54, 33

Cohen J.G., Blakeslee J.P., Ryshov A., 1998, ApJ 496, 808

Côté P., Marzke R.O., West M.J., 1998, ApJ 501, 554

Couture J., Harris W.E., Allwright J.W.B., 1990, ApJS 73, 671

Djorgovski S., Santiago B.X., 1992, ApJ 391, L85

Faber S.M., Tremaine S., Ajhar E., et al., 1997, AJ 114, 1771

Forbes D.A., Brodie J.P., Grillmair C.J., 1997, AJ 113, 1652

Geisler D., Lee M.G., Kim E., 1996, AJ 111, 1529

Harris W.E., 1991, ARA&A 29, 543

Harris W.E., 1996, McMaster database,
    http://visier.u-strasbg.fr/viz-bin/Cat?VII/195

Harris W.E., van den Berg S., 1981, AJ 86, 1627

Kauffmann G., 1996, MNRAS 281, 487

Kauffmann G., Charlot S., 1998, MNRAS 294, 705

Kissler-Patig M., 1997, A&A 319, 83

Kissler-Patig M., Kohle S., Hilker M., et al., 1997, A&A 319, 470

Kissler-Patig M., Brodie J.P., Schroder L.L., et al., 1998a, AJ 115, 105

Kissler-Patig M., Forbes. D.A., Minniti D., 1998b, MNRAS 298, 1123

Kormendy J., Bender R., 1996, ApJ 464, L119

Landolt A., 1992, AJ 104, 340

Larson R., 1975, MNRAS 173, 671

Lauer T.R., Faber S.M., Holtzman J.A., et al., 1991, ApJ 369, L35

Lee M.G., Geisler D., 1993, AJ 106, 493

Michard R., Marchal J., 1994, A&AS 105, 481

Miller G.E., Scalo J.M., 1979, ApJS 41, 513

Neilsen E.H., Tsvetanov Z.I., 1999, astroph/9902164

Paturel G., Andernach L., Bottinelli L., et al., 1997, A&AS 124, 109

Pei Y.C, 1992, ApJ 395, 130

Perelmuter J.M., Racine R., 1995, AJ 109, 1055

Peterson B.A., Ellis R.S., Kibblewhite E.J., et al., 1979, ApJ 233, L109

Pryor C., Meylan G., 1993, Structure and Dynamics of Globular Clus-
    ters. ASP Conf Series vol. 50, 357

Schweizer F., 1997, The Nature of Elliptical galaxies. ASP Conf Series
    vol. 116, 447

Schweizer F., Seitzer P., 1992, AJ 104, 1039

Secker J., Geisler D.,McLaughlin D.E., Harris W.E., 1995, AJ,
    109,1019

Tully R.B., 1988, Nearby Galaxies Catalog. Cambridge University
    Press

Tyson J.A., 1988, AJ 96, 1

Worthey G., 1994, ApJS 95, 107

Zepf S.E., Ashman K.M., Geisler D., 1995, ApJ 443, 570